

# Mechanism of Stress Corrosion Cracking of Face-Centered-Cubic Alloys

著者	TAKANO Michinori, SHIMODAIRA Saburo
journal or publication title	Science reports of the Research Institutes, Tohoku University. Ser. A, Physics, chemistry and metallurgy
volume	18
number	特別号
page range	116-128
year	1966
URL	<a href="http://hdl.handle.net/10097/27308">http://hdl.handle.net/10097/27308</a>

# Mechanism of Stress Corrosion Cracking of Face-Centered-Cubic Alloys\*

Michinori TAKANO and Saburo SHIMODAIRA

(Received May 19, 1966)

## Synopsis

The stress corrosion behaviours of austenitic stainless steels, Inconel and a 70Cu-30Zn alloy in corrosive environments were investigated with thin-foil and bulk specimens. In order to study the segregation of solute atoms in austenitic stainless steels, Instron tensile tests were carried out at 200°C and at a room temperature. The tarnished surface film obtained in Mattsson's solution at pH 7.4 was also examined by electron diffraction method.

The mechanism of the nucleation of transgranular stress corrosion cracking of austenitic stainless steels in a boiling 42% MgCl<sub>2</sub> aqueous solution is different from that of the propagation.

The surface film has an important role in the intergranular stress corrosion cracking of  $\alpha$ -brass in ammonia aqueous solutions, and the initiation of micro pits (preferential dissolution at the fresh slip steps) is not directly associated with the crack nucleation and its propagation.

## I. Introduction

On the mechanism of stress corrosion cracking of alloys in corrosive environments, two principal hypotheses have been proposed: one assumes entirely electrochemical process and the other supposes alternative electrochemical and mechanical process. An important advance in this field has recently been done by the transmission electron-microscope technique with thin-foil specimens, but just little is known about the detailed mechanism.

Bassett and Edeleanu<sup>(1)</sup> were the first to apply electron microscopy to the study of stress corrosion. They observed micro pits produced during the deformation of  $\alpha$ -brass in an ammonia solution, but could not verify the relationship between the micro pits and crystallographic imperfections.

Recently, by the aid of electron microscope, it has been clearly shown that the stress corrosion cracking susceptibility of austenitic stainless steels<sup>(2)-(9)</sup>,

\* The 1249th report of the Research Institute for Iron, Steel and Other Metals.

- (1) G.A. Bassett and C. Edeleanu, *Physical Metallurgy of Stress Corrosion Fracture*, Interscience, New York, (1959), p. 117.
- (2) R. Stickler and S. Barnartt, *J. Electrochem. Soc.*, **109** (1962), 343.
- (3) S. Barnartt, R. Stickler and D. Van Rooyen, *Corrosion Science*, **3** (1963), 9.
- (4) P.R. Swann, *Corrosion*, **19** (1963), 102.
- (5) M. Takano, H. Hashimoto, W. Suëtaka and S. Shimodaira, *J. Japan Inst. Metals*, **28** (1964), 237.
- (6) M. Takano and S. Shimodaira, *J. Japan Inst. Metals*, **29** (1965), 553.
- (7) D.L. Douglass, G. Thomas and W.R. Roser, *Corrosion*, **20** (1964), 15.
- (8) D. Tromans and J. Nutting, *Corrosion*, **21** (1965), 143.
- (9) N. Ohtani and R.A. Dodd, *Corrosion* **21** (1965), 161.

copper alloys<sup>(4),(7)-(10)</sup> and magnesium alloys<sup>(4),(10)</sup> relates closely to crystallographic imperfections. On the initiation of stress corrosion cracking in austenitic stainless steels, the following results have been reported<sup>(6)</sup>: Dislocations distributed in a planar arrangement and only slip steps which were formed continuously under the applied stress in corrosive environments reacted as active sites. The present study is an extension of the previous electron-microscopic studies<sup>(5),(6)</sup> and concerned with the stress corrosion of austenitic stainless steels in a boiling 42% MgCl<sub>2</sub> aqueous solution and of a 70Cu-30Zn alloy in Mattsson's solution (0.05M/L CuSO<sub>4</sub>+0.5M/L (NH<sub>4</sub>)<sub>2</sub>SO<sub>4</sub>). The stress corrosion behaviours of thin-foil and bulk specimens in corrosive environments were examined by electron microscopy and electron diffraction method. Further, the segregation and the precipitation of alloying elements in austenitic stainless steels were examined with Instron tensile test machine.

## II. Experimental procedures

The results of chemical analyses of specimens are listed in Table 1.

Table 1. Chemical composition of test alloys.

	C	Cr	Ni	N	Mn	Si	Fe	Cu	Pb	Zn
Steel A	0.008	17.02	10.20	0.011			balance			
Steel B	0.009	17.18	9.92	0.22			balance			
Steel C	0.13	18.09	8.08	0.053			balance			
Inconel	0.04	16.07	72.09		1.00	0.72	9.99			
Brass							0.003	70.02	0.006	balance

The thin-foil samples were prepared by cold rolling to 0.1 mm in thickness. The samples of the austenitic stainless steels and the Inconel were annealed at 1050°C in vacuum, and that of the 70Cu-30Zn alloy were annealed at 600°C in vacuum, wrapping in thin-foil of the same composition. The deformation procedure of electropolished thin-foil specimens in corrosive environments was performed in the same way as in the previous paper.<sup>(6)</sup>

Specimens for the stress corrosion cracking test and the observation of stress corrosion behaviours by a replica technique were prepared as rectangular slabs, 60×6.5×2.0 mm for stainless steels, 60×6.5×1.5 mm for Inconel and 60×7.0×1.2 mm for brass, and annealed at 1050°C in vacuum for stainless steel and Inconel, and at 600°C for brass. During the annealing, the brass specimens were buried compactly in the mixture of carbon powders and its flakes to prevent them from dezincification.

The application of stress to these bulk specimens was performed by a three point bend-beam system. The solutions used for corroding the alloys are shown in Table 2.

(10) H.W. Pickering and P.R. Swann, *Corrosion*, **19** (1963), 373.

Table 2. Solutions used for the stress corrosion tests of thin-foil and bulk specimens.

	Boiling 42% MgCl <sub>2</sub> aqueous solution (Solution B)	3% NaCl aqueous solution (pH 1.6) at room temperature (Solution A)	Mattsson's solutions (pH 2.0, 7.4 and 10.0)
Steel A	bulk	bulk	
Steel B	thin-foil* and bulk	thin-foil and bulk	
Inconel	thin-foil and bulk		
Brass			thin-foil and bulk

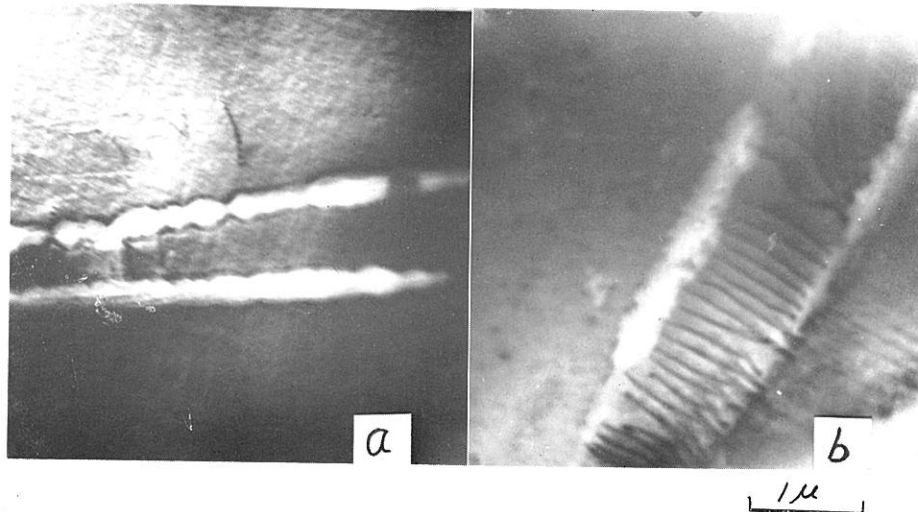
\* ref. (6)

### III. Results and discussion

#### 1. Stainless steel and Inconel

The stress corrosion of the thin-foil specimens of a Steel B was examined in a 3% NaCl aqueous solution (pH 1.6) (Solution A) at room temperature and that of the Inconel was observed in a boiling 42% MgCl<sub>2</sub> aqueous solution (Solution B). Traces of preferential microattacks obtained for the Steel B in the Solution A and for the Inconel in the Solution B are shown in Phots. 1 (a) and (b), respectively. These micrographs show that the micro corrosion trenches result from preferential corrosion along the slip steps caused by dislocation movement under the applied stress. These pitting traces are similar to that of the Steel B obtained in the Solution B.<sup>(6)</sup>

It is well known that the Steel B in the Solution B is susceptible to transgranular cracking and the Steel B in the Solution A and the Inconel in the Solution

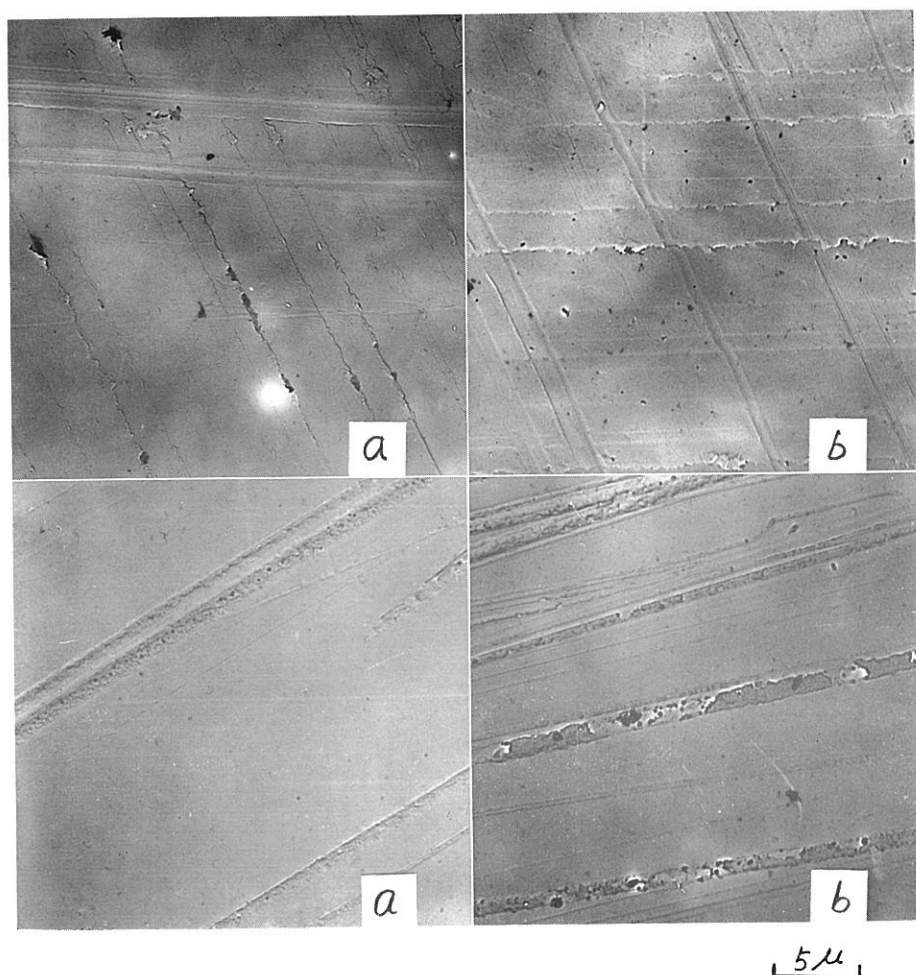


Phot. 1. Preferential microattack at fresh slip steps obtained in deformed thin-foil specimens within corrosive environments for 3 min.

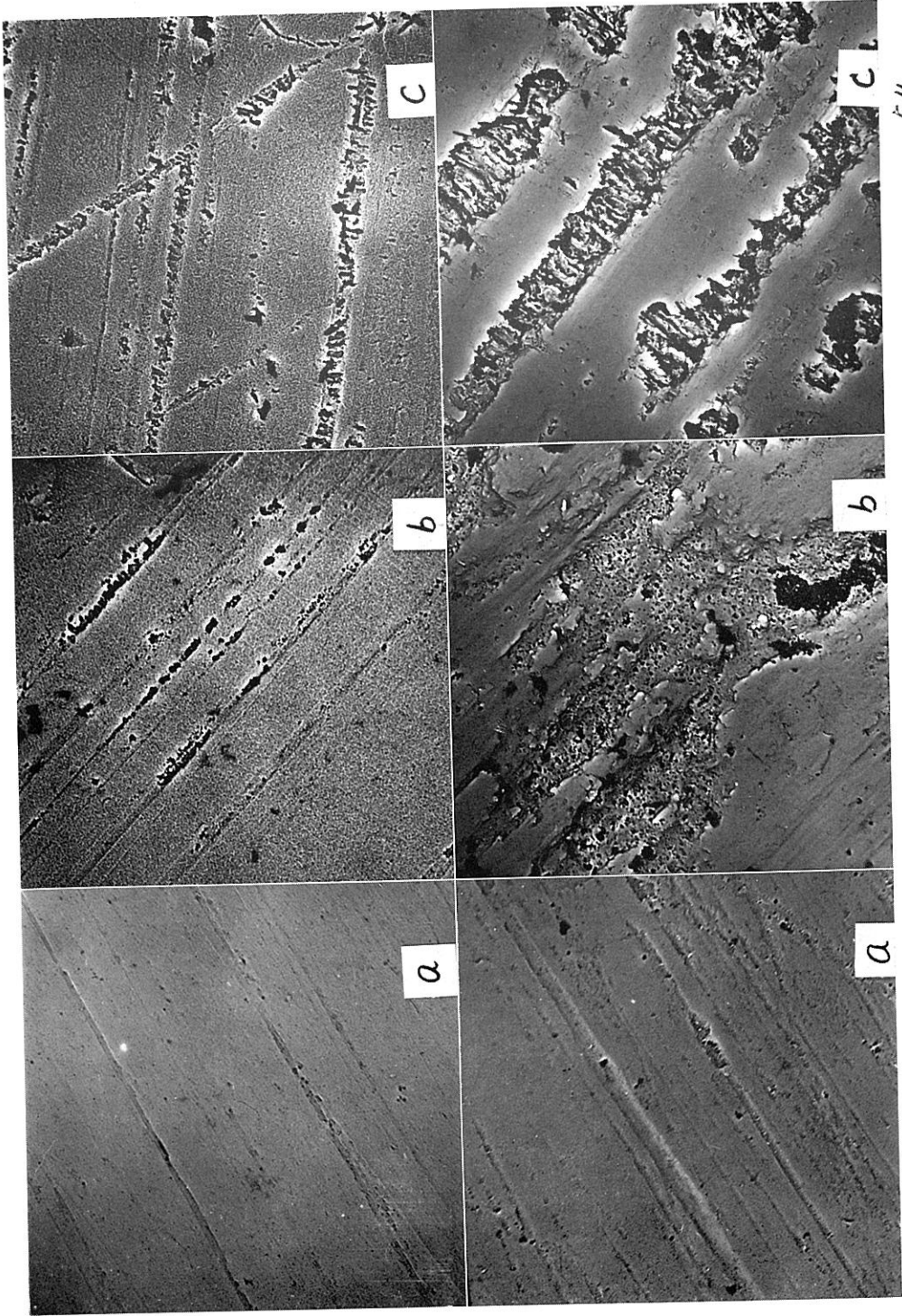
(a) Steel B in Solution A, (b) Inconel in Solution B.

B are unsusceptible to the transgranular cracking. No difference in the initiation stage of stress corrosion, however, could be recognized in the above three cases. The preferential microattacks along fresh slip steps would be controlled by pH, ion species, temperature and some other factors. Therefore, the preferential dissolution at fresh slip steps, as shown in Phot. 1, is considered to be the necessary condition for the nucleation of transgranular cracking of austenitic stainless steels, but not the sufficient condition for crack propagation.

It is important to study how the pits nucleated in the regions of crystallographic defects penetrate into the bulk specimens. The corrosion behaviours of bulk specimens, therefore, were examined as the function of time by the replica technique. Corrosion traces of the Steel A and B in the Solution A are shown in Photos. 2 (a) and (b), that of Inconel, Steel A and B in the Solution B are



Phot. 2. Corrosion traces of (a) Steel A and (b) Steel B obtained in stress corrosion test of bulk specimens in Solution A. Upper; 5 min. Lower; 120 min.



Phot. 3. Corrosion traces obtained in stress corrosion test of bulk specimens in Solution B.

(a) Inconel, Upper; 5 min, Lower; 24 hr, (b) Steel A and (c) Steel B, Upper; 5 min., Lower; 150 min.

shown in Photos. 3 (a), (b) and (c), respectively. The Photos. 2 and 3 (a) show that the initial micropits on the slip steps grow scarcely and cracking does not occur. Photos. 3 (b) and (c), on the other hand, show that the nucleated corrosion trenches proceed into the bulk specimens with increasing exposure time, suggesting transgranular cracking.

Swann and Pickering<sup>(11)</sup>, Uhlig and Sava<sup>(12)</sup> suggested that the segregation of solute atoms in the austenitic stainless steels might be possible at 150°C (this temperature corresponds to that of a boiling 42% MgCl<sub>2</sub> aqueous solution). Chemical compositions in the coarse slip planes and in the vicinity of the planes, therefore, would be different from that in the surrounding regions, and corrosion extends into the bulk specimens along slip planes by electrochemical attack. Hence, the corrosion along the restricted slip steps in the Steel B is particularly considerable, but in the case of the Steel A, the corrosion penetration into the bulk is less remarkable, even if the exposure time is prolonged, and microattacks along original slip steps tend to extend over the bulk surface. The difference between the corrosion behaviours of the Steel A and B in the Solution B can be attributed to the characteristics of dislocation distributions in the alloys, and probably depends on the segregation of solute atoms associated with dislocation arrangements.

Phot. 3 (a) suggests that the solute atoms in the Inconel may not segregate or, even if the segregation occurs at this temperature, these segregated regions may have low chemical activity in the Solution B. It can be considered from Phot. 2 that the probability of segregation in the stainless steels at a room temperature is generally very small (this is responsible for stress-strain curves described later). Therefore, the initial microattack would not proceed into the bulk with increasing time.

Aswegen et al.<sup>(13)</sup> have reported the occurrence of precipitation and segregation at stacking faults in aged stainless steel containing niobium, and Douglass et al.<sup>(14)</sup> have confirmed the preferential precipitation of nitride on the slip planes in aged stainless steel containing nitrogen. Swann and Pickering<sup>(11)</sup>, Uhlig and Sava<sup>(12)</sup> have reported the probability of segregation of solute atom in austenitic stainless steels. In the present study, the behaviours of solute atoms in bulk specimens were investigated by a TT-CM-L type Instron tensile testing machine.

Fig. 1 shows the stress-strain diagrams of the Steel A, B and C at a constant strain rate of 0.05%/min. at 200°C in air, and of the Steel B at the same strain rate at a room temperature. Regarding Steel B and C containing a large amount of nitrogen and carbon, respectively, the remarkable steps were seen in

(11) P.R. Swann and H.W. Pickering, *Corrosion*, **19** (1963), 369.

(12) H.H. Uhlig and J. P. Sava, *Corrosion Science*, **5** (1965), 291.

(13) J.S.T. Van Aswegen, P.W.K. Honeycombe and D.H. Warrington, *Acta Met.*, **12** (1964), 1.

(14) D.L. Douglass, G. Thomas and W.R. Roser, *Corrosion*, **20** (1964), 15.

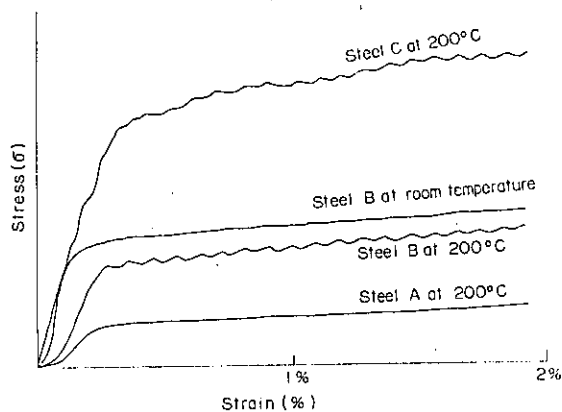


Fig. 1. Stress-strain curves observed in Steel A, Steel B and Steel C elongated at a constant strain rate of 0.05%/min at 200°C and at room temperature in air.

$\sigma$ - $\epsilon$  curves at 200°C, but in the Steel A containing nitrogen and carbon in low amount, this phenomenon was detected in the slightest degree. These steps can probably be attributed to the interaction of solute atoms and crystallographic imperfections<sup>(11)</sup>. The steps obtained in the Steel B at 200°C, however, were not seen at a room temperature. These results are in good agreement with that of Uhlig and Sava<sup>(12)</sup>, which suggested that the segregation of solute atoms would take place at about 200°C.

From these results, it is deduced that the solute atoms participating in the propagation of the transgranular stress corrosion in austenitic stainless steels may segregate in the vicinity of slip planes, and that such a segregation may be sufficient to accelerate an electrochemical reaction. This process is, namely, a sort of mechanochemical reaction.

From the results of the electron-microscopic observations of corrosion behaviours and the Instron tensile tests, the transgranular stress corrosion cracking of the austenitic stainless steel would be nucleated and propagated if the following conditions are satisfied:

- (1) The dislocations distribute in a planar structure.
- (2) Only the fresh slip steps are chemically active, and are attacked preferentially in corrosive environments.
- (3) During the growth of particular slip steps in plastic deformation, solute atoms segregate on the slip planes by moving dislocation and by the creation of vacancies which accelerate the diffusion.
- (4) The segregated regions are electrochemically active against the surrounding matrix in corrosive environments.

When the above mentioned conditions are satisfied, the transgranular stress corrosion cracking would be proceeded by electrochemical reaction along the segregated regions (that is,  $\{111\}$  planes).



## 2. 70Cu-30Zn alloy

The stress corrosion cracking tests of the 70Cu-30Zn alloy were performed in Mattsson's solutions at various pH values (2.0, 7.4 and 10.0). At pH 7.4, the specimens were covered with the black surface film and intergranular cracking occurred after 23 to 24 hr. At pH 2.0, the specimens were scarcely corroded, but were severely corroded without the formation of surface film at pH 10.0, and were not cracked at either pH within 1 week.

Mattsson<sup>(15)</sup> has reported the electrochemical reactions of a 63Cu-37Zn alloy in solutions containing copper sulphate, ammonium sulphate and ammonium hydroxide in the pH range of 2.0 to 11.2. His results, generally, agree well with the results of the corrosion behaviours in the present experiment. From the electron diffraction analysis of the intergranular cracking surface, it was found that the surface film developed in the Mattsson's solution at pH 7.4, consisted only of  $\text{Cu}_2\text{O}$ . This result is in good agreement with that of Forty and Humble<sup>(16)</sup>, and of McEvily and Bond.<sup>(17)</sup>

It is generally known that the dislocation arrangements in Cu-Zn alloys have a tendency to vary from a cellular to a planar structure as the zinc content is increased.

Swann<sup>(4)</sup> has explained the characteristics of inter- and transgranular stress corrosion cracking in Cu-Zn alloys with the generally accepted relation between the variation of dislocation arrangements and that of stacking fault energy. The type of stress corrosion cracking in Cu-Zn alloys, however, depends also on the corrosive environments or on the applied stress. It seems difficult to elucidate the mechanism of cracking only by the distributions of dislocation.

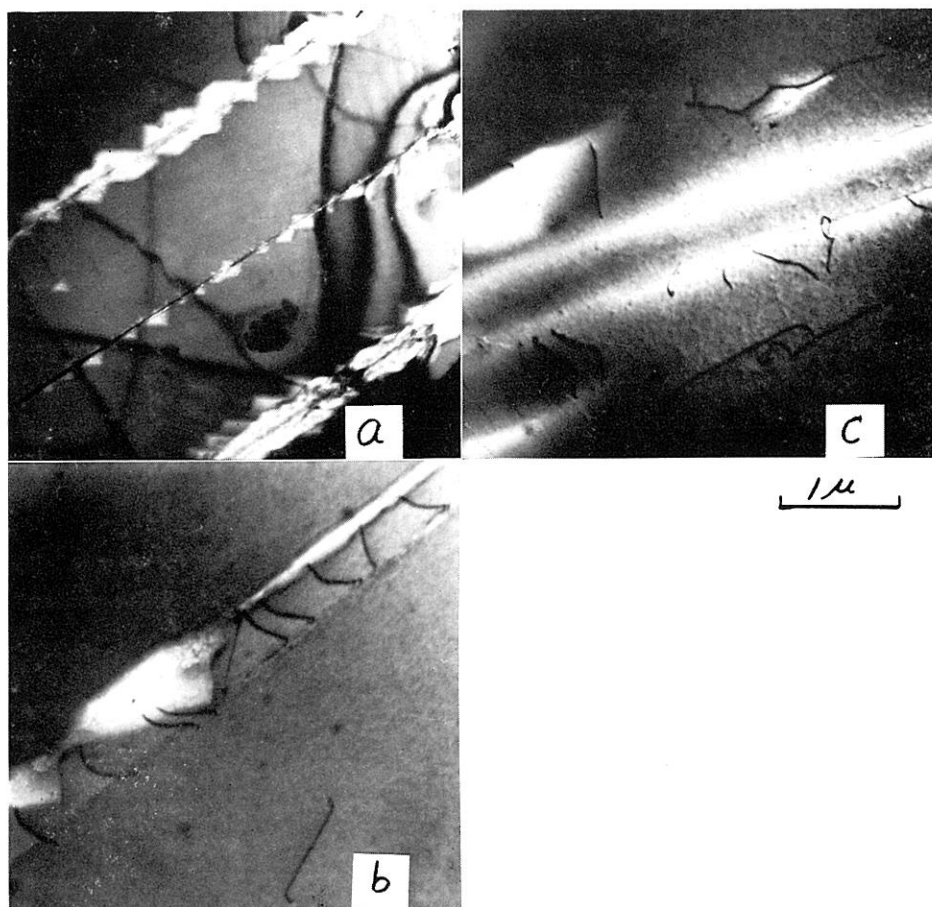
In the present investigation, the dislocations seen in a 5 per cent deformed 70 Cu-30Zn alloy are restricted on the particular slip plane, and the coarse slip steps are produced during the plastic deformation.

The traces of micro pits obtained from the deformed thin-foil specimens in Mattsson's solutions at pH 2.0, 7.4 and 10.0 are shown in Phots. 4 (a), (b) and (c), respectively. Although the stress corrosion behaviours of bulk specimens depended extremely on the pH values, the preferential micro dissolution of thin-foil specimens occurred predominantly at the fresh slip steps at any pH value as seen in Phot. 4. Tromans and Nutting<sup>(8)</sup> have reported that the preferential attacks of a 70Cu-30Zn thin-foil specimens in the Mattsson's solution at pH 7.3 occurred at the grain boundaries and at the individual dislocations adjacent to the grain boundaries, and that these micro attacks are associated directly with the intergranular microcracking. In the present experiment, however, the micro pits obtained at pH 7.4 are not associated with the dislocations adjacent to the grain boundaries as shown in Phot. 4 (b), but nucleated at the slip steps within the

(15) E. Mattsson, *Electrochimica Acta*, **3** (1961), 279.

(16) A.J. Forty and P. Humble, *Phil. Mag.*, **8** (1963), 247.

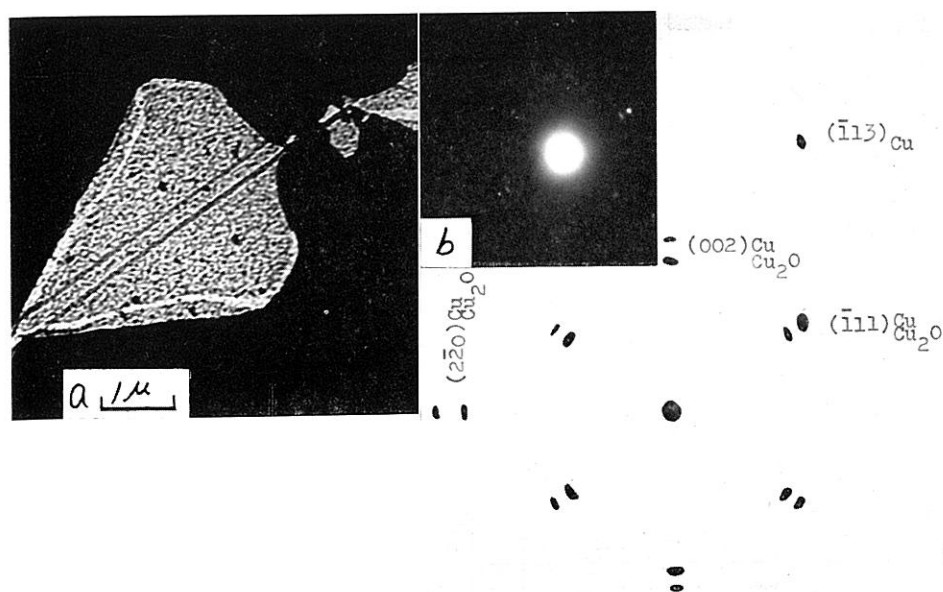
(17) A.J. McEvily and A.P. Bond, *J. Electrochem. Soc.*, **112** (1965), 131.



Phot. 4. Preferential microattack at fresh slip steps obtained in deformed thin-foil 70Cu-30Zn alloy in Mattsson's solution for 3 min, at (a) pH 2.0, (b) pH 7.4 and (c) pH 10.0.

crystal grains and formed micro attacked trenches, extending, at the same time, over the brass surface. A typical example of surface-extended corrosion is shown in Phot. 5 (a), and the selected area diffraction pattern from this region is shown in Phot. 5 (b). This pattern shows that the corrosion products of preferentially attacked region consist of Cu and  $\text{Cu}_2\text{O}$ , and that  $\text{Cu}_2\text{O}$  develops epitaxially on the dezincified copper metal. Zn and ZnO were not detected in the corroded thin-foil specimen. The existence of  $\text{Cu}_2\text{O}$  and Cu layers in the thin-foil specimen agrees with the result that the surface film obtained from the cracked brass at pH 7.4 consisted of  $\text{Cu}_2\text{O}$ . From these results, it seems that the thick surface layers of  $\text{Cu}_2\text{O}$  and Cu play an important role in intergranular stress corrosion cracking of brass in aqueous solutions of ammonia.

If the aspect of extension of the initial micro pits at the crystallographic defects can be observed, the results should be very effective for studying the



Phot. 5. (a) Typical example of surface-extended corrosion obtained in deformed thin-foil 70Cu-30Zn alloy in Mattsson's solution at pH 7.4 for 3 min.  
 (b) Selected area diffraction pattern from surface-extended corroded region. Showing epitaxial relation between  $Cu_2O$  and dezincified copper metal.

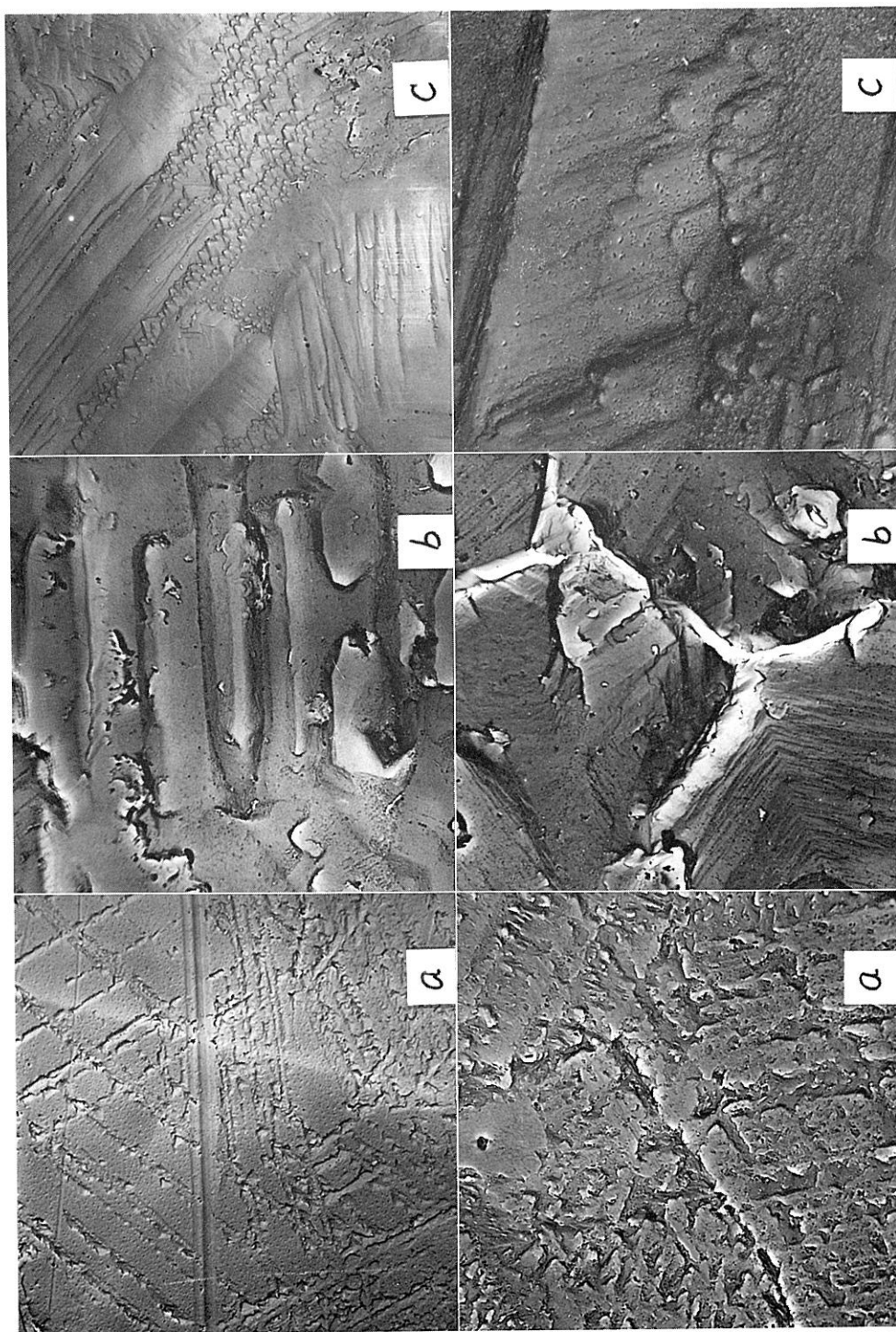
mechanism of stress corrosion cracking. The corrosion behaviours of bulk specimens varying with the exposure time were, therefore, examined by the replica technique. The stress corrosion behaviours of the bulk specimens at each pH value after 5 min and 120 min are shown in Photos. 6 (a), (b) and (c).

Photos. 6 (a), (b) and (c) show the following characteristics: At pH 2.0, the stress corrosion progresses scarcely, the initial micro attacked trenches at slip steps still remain even after 120 min, and the propagation of crack is difficult. At pH 7.4, the micro pits extend over the specimen surface forming  $Cu_2O$  and Cu layers (5 min). After brass surface are entirely covered with these layers, corrosion proceeds along the grain boundaries, giving rise to intergranular cracking (120 min). At pH 10.0, the corrosion rate is very high, the original surface topography of bulk specimen is not preserved and the general corrosion is observed (5 min).

From these results, the mechanism of the intergranular stress corrosion cracking of the 70Cu-30Zn alloy in aqueous solutions of ammonia is considered as follows:

1. Fresh coarse slip steps produced by the movement of dislocations under the applied stress are preferentially corroded, and the surface films of  $Cu_2O$  and Cu are produced. (Fig. 2 (a)).

2.  $Cu_2O$  and Cu films developed on the slip steps act as the electrochemical cathode to the brass substrate and accelerate the electrochemical corrosion. In



Phot. 6. Corrosion traces of 70Cu-30Zn alloy obtained in stress corrosion test in Mattsson's solution at (a) pH 10.0, Upper; 5 min, Lower; 120 min. 7.4 and (c) pH 2.0, (b) pH 7.4 and (c) pH 10.0, Upper; 5 min, Lower; 120 min.

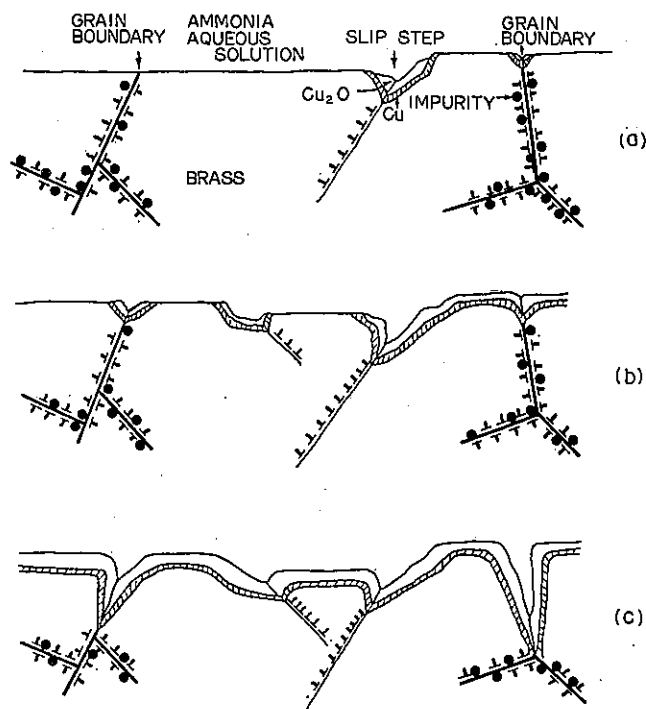


Fig. 2. Schematic representation of intergranular stress corrosion cracking of brass in ammonia aqueous solution.

- (a) Showing the preferential microattack at slip step.
- (b) Microattacks began to extend over the brass surface and the movement of dislocations at coarse slip plane is locked by  $\text{Cu}_2\text{O}$  and Cu layers.
- (c) After brass surface is covered with these layers, crack propagates along grain boundaries.

this stage, the thick films exist in the region of the original slip steps, so that the movement of dislocations on the original slip planes is locked. Other slip steps could be, consequently, formed in uncorroded regions, and these new slip steps would have the same behaviours as those shown in Fig. 2 (a) (Fig. 2 (b)).

3. The brass surface is thus covered with films of  $\text{Cu}_2\text{O}$  and Cu of thick and large grain size. In this stage, the movement of dislocations on the emergent slip planes are almost locked by the surface films. The dislocations and vacancies, therefore, are more easily absorbed in the grain boundaries than when the brass surface are uncovered with  $\text{Cu}_2\text{O}$  and Cu films, relieving the stress. The grain boundaries contain dislocations and impurities in high density, and the disturbance would increase with increasing absorption of dislocation under the presence of the surface films, so that the chemical reaction in grain boundaries becomes more active, and the corrosion is more accelerated. The stress corrosion cracking, thus, propagates along the grain boundaries by corrosion (Fig. 2 (c)).

Concerning the chloride cracking in the austenitic stainless steels, the micro pits nucleated at the slip steps continuously develop, resulting in the transgranular cracking by the effect of segregation. However, regarding the ammonia cracking in  $\alpha$ -brass, as mentioned above, the initial micro pits nucleated at the fresh slip steps do not grow into the crack by themselves, but surface films are formed at these chemically active sites. These films behave as the cathode, and are uniformly developed on the brass substrate. These surface films would lock the movement of dislocations on the emergent slip planes, and the grain boundaries would become chemically active sites.

### Conclusion

The stress corrosion behaviours of the thin-foil specimens of a nitrogen rich stainless steel in a 3% NaCl aqueous solution (pH 1.6) at a room temperature and of Inconel in a boiling 42% MgCl<sub>2</sub> aqueous solution are similar to that of a nitrogen rich stainless steel in a boiling 42% MgCl<sub>2</sub> aqueous solution. From the results of the observation of the stress corrosion for bulk specimens with varying exposure time by the replica method and of the Instron tensile tests, an occurrence of segregation is concluded in the stress corrosion susceptible alloy. The mechanism of nucleation of the transgranular stress corrosion cracking in the austenitic stainless steels is different from that of the propagation.

Regarding the stress corrosion of 70Cu-30Zn alloy in Mattsson's solutions, no difference was recognized about the initiation of micro pits for the pH values studied, that is, the predominant formation of micro pits was observed at slip steps in all cases. At pH 7.4, however, the regions of micro pits consisted of Cu<sub>2</sub>O and Cu layers, which behaved as the electrochemical cathode, and the brass substrate was covered with these layers. They have the effect of locking the movement of dislocations on the emergent slips. Consequently, the grain boundaries are much more chemically activated than those without the surface layers, forming the path of crack in grain boundaries.

Initiation of micro pits (preferential dissolution of crystal defects) was not directly associated with the nucleation and the growth of intergranular cracking in  $\alpha$ -brass in ammonia aqueous solutions.